applied sciences

MDPI

Article

A Study on Enhancing the Visual Fidelity of Aviation Simulators Using WGAN-GP for Remote Sensing Image Color Correction

Chanho Lee [1,†], Hyukjin Kwon [1,†], Hanseon Choi [1], Jonggeun Choi [1], Ilkyun Lee [2], Byungkyoo Kim [3], Jisoo Jang [4,5] and Dongkyoo Shin [4,5,*]

[1] Department of Defense Artificial Intelligence Applications, Seoul National University of Science and Technology, Seoul 01811, Republic of Korea; cksgh1211@seoultech.ac.kr (C.L.); kwonhj@seoultech.ac.kr (H.K.); gkstjls@seoultech.ac.kr (H.C.); choijon1@seoultech.ac.kr (J.C.)
[2] Avionics Software Development Center of Republic of Korea Air Force Logistics Command, Seosan 32024, Republic of Korea; simdb@mnd.go.kr
[3] AI Convergence Center, Sungkyunkwan University, Suwon 16419, Republic of Korea; kbkidid@skku.edu
[4] Department of Computer Engineering, Sejong University, Seoul 05006, Republic of Korea; werkki96@gmail.com
[5] Department of Convergence Engineering for Intelligent Drones, Sejong University, Seoul 05006, Republic of Korea
* Correspondence: shindk@sejong.ac.kr
† These authors contributed equally to this work.

Abstract: When implementing outside-the-window (OTW) visuals in aviation tactical simulators, maintaining terrain image color consistency is critical for enhancing pilot immersion and focus. However, due to various environmental factors, inconsistent image colors in terrain can cause visual confusion and diminish realism. To address these issues, a color correction technique based on a Wasserstein Generative Adversarial Network with Gradient Penalty (WGAN-GP) is proposed. The proposed WGAN-GP model utilizes multi-scale feature extraction and Wasserstein distance to effectively measure and adjust the color distribution difference between the input image and the reference image. This approach can preserve the texture and structural characteristics of the image while maintaining color consistency. In particular, by converting Bands 2, 3, and 4 of the BigEarthNet-S2 dataset into RGB images as the reference image and preprocessing the reference image to serve as the input image, it is demonstrated that the proposed WGAN-GP model can handle large-scale remote sensing images containing various lighting conditions and color differences. The experimental results showed that the proposed WGAN-GP model outperformed traditional methods, such as histogram matching and color transfer, and was effective in reflecting the style of the reference image to the target image while maintaining the structural elements of the target image during the training process. Quantitative analysis demonstrated that the mid-stage model achieved a PSNR of 28.93 dB and an SSIM of 0.7116, which significantly outperforms traditional methods. Furthermore, the LPIPS score was reduced to 0.3978, indicating improved perceptual similarity. This approach can contribute to improving the visual elements of the simulator to enhance pilot immersion and has the potential to significantly reduce time and costs compared to the manual methods currently used by the Republic of Korea Air Force.

Keywords: color enhancing; Wasserstein GAN with Gradient Penalty; remote sensing images; aviation simulators

Citation: Lee, C.; Kwon, H.; Choi, H.; Choi, J.; Lee, I.; Kim, B.; Jang, J.; Shin, D. A Study on Enhancing the Visual Fidelity of Aviation Simulators Using WGAN-GP for Remote Sensing Image Color Correction. *Appl. Sci.* **2024**, *14*, 9227. https://doi.org/10.3390/app14209227

Academic Editor: Pedro Couto

Received: 27 August 2024
Revised: 9 October 2024
Accepted: 10 October 2024
Published: 11 October 2024

1. Introduction

Aviation simulators have become essential tools for pilot training by closely replicating real-world flight environments. As the cost of real-world flights increases alongside technological advancements in aircraft, the utilization of simulators becomes even more critical. High fidelity is required to enhance simulator immersion, with visuals such as

outside-the-window (OTW) imagery playing a critical role. Additionally, the need for new locations for overseas missions requires simulation training in a variety of environments, making terrain imagery accuracy and consistency critical.

Terrain imagery is a key component of a simulator's visual representation of the Earth's surface features and is primarily obtained through aerial photography and satellite imagery. However, even when the same area is photographed, factors such as seasonal changes, lighting conditions, and cloud cover can lead to irregular terrain images. These irregular terrain images can be aesthetically unpleasant and, as a result, distracting to pilots. Currently, the Republic of Korea (ROK) Air Force requires human intervention in most processes to improve these images, leading to inconsistent results and increased work time.

To address this issue, histogram matching [1–4] has been widely used. This method adjusts the color histogram of the target image to align with the color distribution of the reference image. This method may not fully account for local variations or complex textures, leading to a loss of detail and potentially unnatural results when there are large color differences.

Color transfer [5–8] conveys a specific hue or mood by converting the colors of the target image to match the color statistics (e.g., mean, variance, etc.) of a reference image. This method also risks not preserving the structural features or textures of the image and can result in unnatural outcomes if the color difference is significant.

To overcome these issues, Generative Adversarial Network (GAN)-based color correction techniques [9–13] have been proposed. GANs generate realistic data through adversarial learning between a Generator and a discriminator (later termed a Critic) and can convert irregular colors into consistent ones. However, there is a risk of mode collapse and overfitting for specific data during the learning process, and the loss function has an important impact on learning stability.

In this study, the WGAN-GP (Wasserstein Generative Adversarial Network with Gradient Penalty) [14] was used, which introduces a Gradient Penalty to overcome the limitations of traditional WGAN [15], improving learning stability and efficiency. By redefining the loss function using the Wasserstein distance concept and ensuring the Lipschitz continuity of the Critic, the mode collapse problem is mitigated, leading to more stable training and improved data quality.

Mode collapse, if left unaddressed, can severely impact remote sensing image color correction by causing repetitive color patterns and limited diversity in generated images. This can lead to distorted color distributions that fail to accurately represent the wide variety of textures and conditions present in remote sensing data, compromising the realism needed for applications like aviation simulators [16]. By effectively addressing mode collapse, WGAN-GP ensures that the generated images maintain diverse and accurate color representations, which are crucial for achieving realistic and immersive simulations.

While previous studies have utilized WGAN-GP on whole remote sensing images, there are few studies that have applied WGAN-GP to partial images. In this study, WGAN-GP was applied to partial images using the BigEarth-Net-S2 [17] dataset. This dataset consists of 549,488 Sentinel-2 image patches collected from 10 European countries and contains a wide variety of terrain, seasons, and weather conditions, making it a suitable dataset for training WGAN-GP-based models.

This paper is organized as follows: Section 2 reviews related work, details the dataset and the methodology of the proposed WGAN-GP-based model, Section 4 describes the experiment, and Section 5 discusses the findings. Finally, Section 6 concludes the study and suggests future research directions.

2. Related Works

There has been considerable research on uniformly correcting irregular colors in remote sensing images. These studies have primarily focused on Wallis filters, histogram matching, color transfer, and more recently, GAN-based methods.

In Wallis filter research, Z. Hong et al. [18] proposed optimizing color, luminance, and contrast consistency among multiple remote sensing images by processing the chroma and luminance channels in the YCbCr color space to minimize color differences and used the Wallis transform to optimize luminance and contrast. C. Fan et al. [19] proposed an improved Wallis Dodging method suitable for large-scale super-resolution reconstructed remote sensing images. The algorithm calculates the Wallis filter parameters for each image in a weighted manner and uses a weighted iterative method between adjacent images to reduce spatial error propagation, resulting in a more precise adjustment of color consistency across large-scale images. M. W. Sun et al. [20] proposed using a homomorphic filter along with the Wallis transform to address irregular brightness distribution and color differences. The homomorphic filter adjusts brightness imbalances within the image to resolve the hotspot problem, while the Wallis transform reduces color differences between images to achieve color consistency. A template-based filtering method for seam removal was also employed to address irregularities.

In histogram research, J. Morovic et al. [21] proposed a 3D histogram transformation to more precisely maintain color consistency in images. This method overcomes the limitations of existing 2D histogram transformation and enables high-accuracy color conversion even for images with complex color structures. L. Neumann et al. [22] proposed a method of individually matching histograms of color, brightness, and saturation to naturally transfer color styles between two images.

In color transfer research, Reinhard et al. [23] proposed matching the color distributions by adjusting the mean and standard deviation between the source and target images in the Lab color space, demonstrating that this can produce natural results while maintaining color consistency. F. Pitie et al. [24] performed color transfer by minimizing the difference in the probability density functions between two images in multidimensional space, resulting in more natural and consistent color transfer compared to conventional methods.

In GAN-based research, T. Katayama et al. [25] proposed a color correction technique using GANs to solve the color distortion problem occurring in underwater environments. The proposed method enables more natural and consistent color restoration, significantly improving the accuracy of color correction and object detection in underwater environments. M. Afifi et al. [26] proposed a method to control the color of GAN-generated images using color histograms, which facilitates natural color transfer. Additionally, a new model called ReHistoGAN can realign the colors of an actual image to match the target color histogram.

These related works have presented various approaches to solve the problem of color consistency in remote sensing images. While Wallis filters, histograms, and color transfer methods each have their own advantages, they have also shown limitations in dealing with complex color structures and large-scale images. Recent GAN-based studies have overcome some of these limitations, but challenges remain in learning stability and producing consistent results. In this study, a new approach using a WGAN-GP model is proposed to overcome the limitations of these previous studies.

3. Methods

3.1. Model Architecture

The architecture of the WGAN-GP-based color correction model involves two adversarial components, the Generator (G) and the Critic (C), which are trained simultaneously. The Generator (G) takes, as input, a pair of images, consisting of a reference image (x_{ref}) and a target image (x_{target}), and aims to realistically generate an image ($G(x_{ref}., .x_{target})$) that resembles the reference image (x_{ref}). Meanwhile, the Critic (C) determines whether the input image is the reference image (x_{ref}) or the generated image ($G(x_{ref}., .x_{target})$). The architecture of the WGAN-GP model is illustrated in Figure 1.

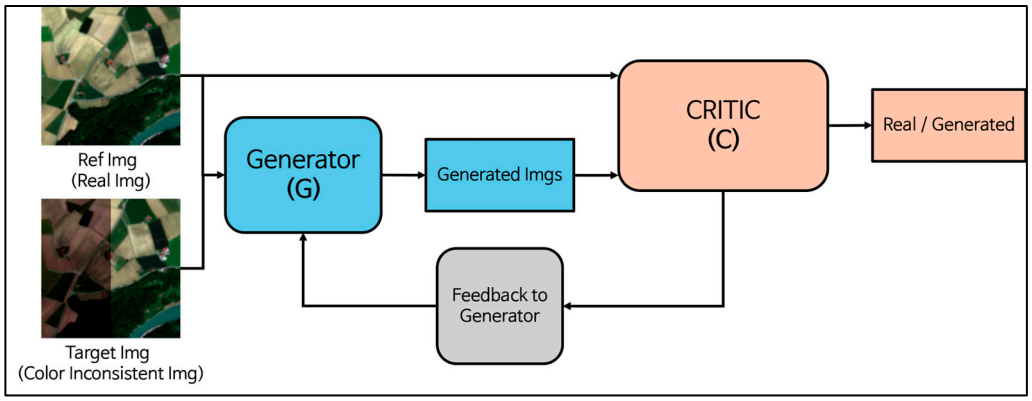

Figure 1. An overview of the architecture of the WGAN-GP model.

The G takes a reference image (x_{ref}) and a target image (x_{target}) as inputs and combines them to create a new image. The architecture of the G used in this study is organized as follows.

To simplify, the G first combines the two input images and applies a series of convolutional layers and activation functions to gradually extract features. In more detail, the G starts by passing the combined images through a 3 × 3 convolutional layer with ReLU activation, which is repeated twice to capture basic patterns. MaxPooling is then applied to reduce the dimensions, summarizing key features. This process is repeated twice, with the number of filters increasing each time to capture more complex details as the resolution decreases. In the next stage, G uses up-sampling to restore resolution, followed by further convolutional layers and ReLU activation to refine the image output. In the final step, a sigmoid function is applied to ensure the output values are within the range [0, 1], as shown in Figure 2a.

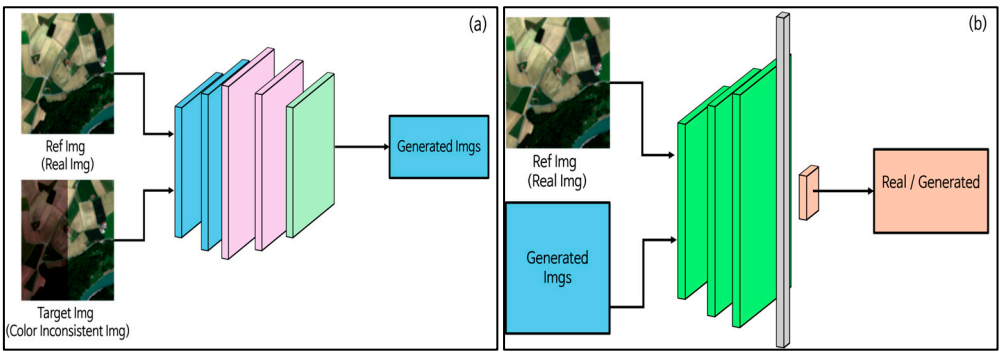

Figure 2. Architecture of the Generator and Critic in the WGAN-GP model. (**a**) Architecture of the Generator (**b**) Architecture of the Critic.

The C is responsible for determining whether the input image is a real image (reference image, x_{ref}) or a generated image ($G(x_{ref}., .x_{target})$). The architecture of C used in this study is organized as follows.

The C follows a similar approach but focuses on differentiating between real and generated images. The input is passed through a 3 × 3 convolutional layer with ReLU activation, followed by MaxPooling to reduce dimensions and extract essential features. This process is repeated three times, with increasing filter numbers to enhance the detection of patterns. Finally, the output is flattened into a vector through a Flatten layer, and a final decision is made, as shown in Figure 2b. To make this process more intuitive, a flowchart explaining each step visually has been included in Figure 1.

3.2. Loss Functions

The loss function of the WGAN-GP model proposed in this paper, which considers both pixel accuracy and the quality of the generated image, is expressed as follows:

$$Loss_{WGAN} = E_{x_{ref}}\left[C\left(x_{ref}\right)\right] - E_{G(x_{ref},x_{target})}\left[C\left(G\left(x_{ref}, x_{target}\right)\right)\right]$$

where $C(x_{ref})$ is the value that the Critic calculates for the reference image (x_{ref}). $C(G(x_{ref}, x_{target}))$ is the value the C calculates for the image generated by the G using the reference image ($.x_{ref}$) and the target image (x_{target}). This value assesses how closely the generated image resembles the real image.

The loss function operates by having the C take both the reference image (x_{ref}) and the generated image $G(x_{ref}, x_{target})$ as inputs, determining which of the two is the real image (x_{ref}) and which is the generated image $G(x_{ref}, x_{target})$.

The G takes a reference image (x_{ref}) and a target image (x_{target}) as inputs and generates an image that reflects the style of the reference image (x_{ref}) while preserving the structure or content of the target image (x_{target}).

The C aims to maximize the value of $C(x_{ref})$ and minimize the value of $C(G(x_{ref}, x_{target}))$, meaning it seeks to evaluate the reference image ($.x_{ref}$) as real and the generated image as not real. Conversely, the G tries to maximize the value of $C(G(x_{ref}, x_{target}))$, aiming for the generated image ($G(x_{ref}., .x_{target})$) to be perceived as a real image.

The model simultaneously learns the color distribution and texture of the target image. In this process, the C evaluates both aspects of color consistency and structure. This learning is crucial in aviation simulators because maintaining the color consistency and structural integrity of terrain images provides pilots with an accurate and immersive training environment. If either the color or texture is not accurately represented, the effectiveness of the aviation simulation could be compromised.

By repeating this process, the G learns to produce images that increasingly reflect the style of the reference image (x_{ref}) while also preserving the content of the target image (x_{target}).

However, it is important to note that while the WGAN-GP model provides superior results in terms of color consistency and texture preservation, it comes with a higher computational cost compared to simpler models such as histogram matching and basic color transfer. Training the WGAN-GP model requires more computational resources, including multiple high-performance GPUs and an extended training time. This makes it suitable primarily for applications where the accuracy and quality of color correction are critical, such as high-fidelity aviation simulators, rather than for use cases where computational efficiency is the priority. By understanding these trade-offs, practitioners can make informed decisions on whether the benefits of WGAN-GP justify its use based on the specific requirements and constraints of their application.

4. Experimental Section

In this section, performance evaluation experiments are conducted to validate the proposed model.

4.1. Datasets

In this study, the BigEarthNet-S2 dataset was used for the color correction of high-resolution remote sensing images. The dataset consists of 115 Sentinel-2 tiles collected from June 2017 to May 2018 across 10 European countries (Austria, Belgium, Finland, Ireland, Kosovo, Latvia, Luxembourg, Portugal, Serbia, and Switzerland). These tiles were atmospherically corrected using the Sentinel-2 Level 2A product creation and formatting tool and were then divided into a total of 549,488 image patches.

Each image patch is associated with a pixel-level reference map and multiple land cover class labels (i.e., multi-label) derived using the latest 2018 CORINE Land Cover

database. The dataset includes a wide range of terrains, seasons, and weather conditions, making it sufficient for training color correction models in various environments.

The BigEarthNet-S2 dataset utilizes imagery collected by the Sentinel-2 satellite, which is part of the European Space Agency's (ESA's) Copernicus project. Sentinel-2 provides a wide range of spectral bands for precise observations of the Earth's surface, and the cloud cover in all Sentinel-2 images is limited to 1% or less to minimize its impact on the results. The spectral bands available in the Sentinel-2 imagery include the following: B01 (coastal aerosol; 60 m), B02 (blue; 10 m), B03 (green; 10 m), B04 (red; 10 m), B05 (vegetation red edge; 20 m), B06 (vegetation red edge; 20 m), B07 (vegetation red edge; 20 m), B08 (near-infrared (NIR); 10 m), B09 (water vapor; 60 m), B11 (short-wave infrared (SWIR); 20 m), B12 (SWIR; 20 m), and B8A (narrow NIR; 20 m). Among these, bands B04, B03, and B02, which correspond to red, green, and blue, were selected to create the RGB image. The choice was made due to their 10 m resolution, which offers an optimal balance between spatial detail and accurate color representation for natural imagery. In this study, a high-resolution RGB image created by combining the red, green, and blue channels (bands 4, 3, and 2) was used as the reference image, as shown in Figure 3.

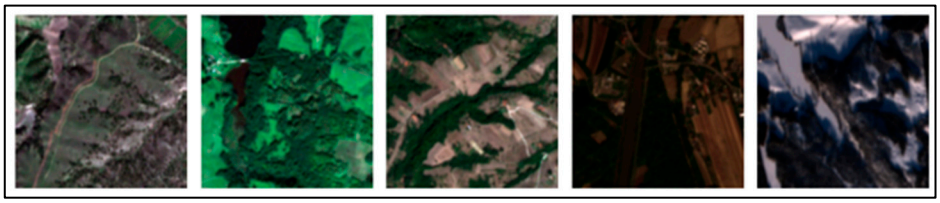

Figure 3. BigEarthNet-S2 RGB images (ref images).

To create the target image, the RGB image was randomly divided in one of the following ways: vertical bisection, diagonal division, three divisions, or four divisions, and then randomly color-adjusted, luminance-adjusted, and contrast-adjusted. Color adjustment was performed by selecting a random value between −30 and +30 to correct the hue and change the ratio of primary colors; luminance adjustment was performed by selecting a random value between −50 and +50 to adjust the overall brightness; and contrast adjustment was performed by selecting a random value between 0.5 and 1.5 to adjust the contrast, as shown in Figure 4. These parameter ranges were determined based on empirical analysis. The chosen values were optimized to provide sufficient variability while maintaining the natural appearance of terrain images, ensuring that the adjustments align with the real-world conditions observed in remote sensing environments. The RGB image and the preprocessed image were then resized to 256 × 256 pixels and normalized to the range [0, 1]. The RGB image and the preprocessed target image were then paired and used for training.

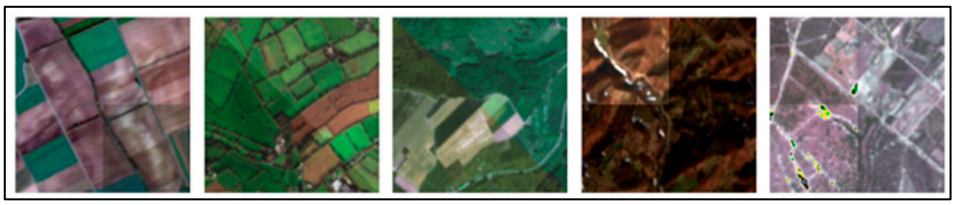

Figure 4. BigEarthNet-S2 preprocessing images (target images).

4.2. Experimental Environment

WGAN-GP was implemented using the TensorFlow framework and the model was trained on three NVIDIA DGX A100 80 GB GPUs. The BigEarthNet-S2 RGB image was used as the reference image, and the preprocessed BigEarthNet-S2 RGB image was used as the target image in the dataset. The weight λ of the Gradient Penalty term, as proposed in the WGAN-GP paper, was set to 10.0. The model was optimized using the Adam opti-

mizer with mini-batches, where the Adam optimizer parameters were set to $\beta 1 = 0.5$ and $\beta 2 = 0.9$. The learning rate for the Generator was set to 1×10^{-4}, and the learning rate for the Critic was set to 5×10^{-5}. The maximum number of epochs was 50, and the batch size was 128. Additionally, the trained model was presented to a terrain imaging expert from the ROK Air Force, who provided feedback on ensuring that important terrain features were not lost during the color conversion process. Based on this feedback, further research was conducted, focusing on the structure of the Generator and Critic and optimizing hyperparameters.

4.3. Results

This section presents the training results of the WGAN-GP model proposed in this paper. The proposed model effectively improved color and texture reproduction through the training process using reference images. The reference images were only used during the model training phase and are not required for the model's actual deployment.

As training progressed, the color and texture of the generated images improved significantly. Initially, the color distribution was irregular, but with continued training, this irregularity gradually decreased, and eventually, the model was able to produce images with increasingly uniform color distribution. Figure 5 shows that the model effectively learned color consistency, and the images generated at each stage of the training gradually became more similar to the ground truth.

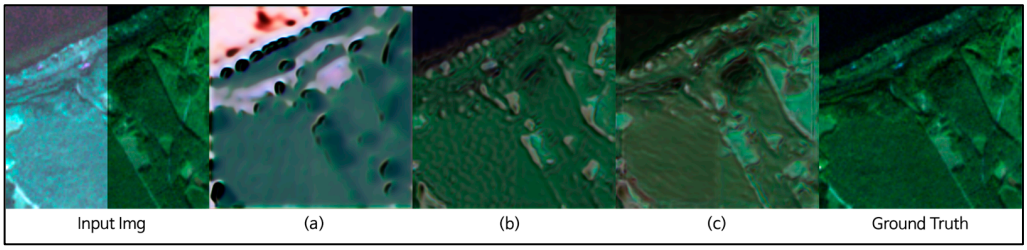

Figure 5. Color matching results of BigEarthNet-S2 RGB images and BigEarthNet-S2 preprocessing images. (**a**) Generated image by model at the early stage of training, (**b**) generated image by model at the mid-stage of training, and (**c**) generated image by fully trained model.

Furthermore, the texture representation in the generated images was significantly improved compared to the initial training phase. In terms of texture reproduction, some unclear areas were observed in the early stages, but as training progressed, more sophisticated and detailed textures emerged. Figure 6 demonstrates that the WGAN-GP-based color correction model effectively learned and reproduced the features of the ground truth texture, showcasing an important result.

To facilitate a clearer understanding of these visual enhancements, Figures 5 and 6 have been annotated with additional labels and captions. Each stage of training is marked to indicate specific improvements in color distribution and texture details, such as reduced color inconsistency, smoother texture transitions, and the emergence of finer details. These annotations guide the viewer through the model's progressive learning, illustrating the effectiveness of the WGAN-GP approach in refining both color and texture throughout the training process. Therefore, the WGAN-GP-based color correction model proposed in this study demonstrates strong performance not only in maintaining color consistency but also in the precise reproduction of textures.

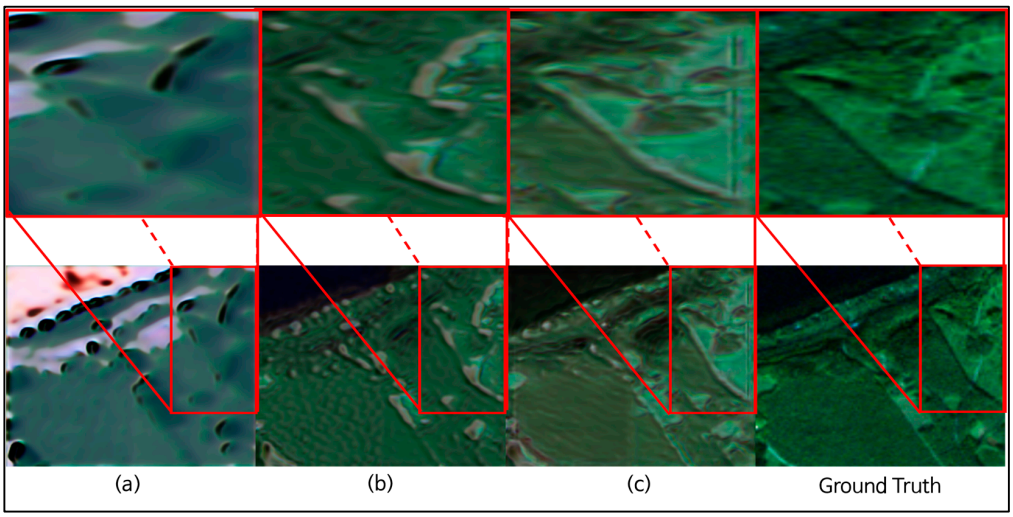

Figure 6. Precise texture reproduction results. (**a**) Generated image by model at the early stage of training, (**b**) generated image by model at the mid-stage of training, and (**c**) generated image by fully trained model.

4.4. Ablation Study

To evaluate the effectiveness of the WGAN-GP model, ablation experiments were conducted by comparing it with a modified model where only the gradient penalty (GP) was added. This experiment aimed to specifically assess the impact of each component on the model's performance and to highlight the advantages of the WGAN-GP architecture compared to conventional methods. The results yielded the following insights and challenges:

Firstly, when the Gradient Penalty (GP) was added to a standard GAN model alone, it helped control the gradient of the Critic, improving the stability of the training process. However, it did not fundamentally resolve the existing issues inherent in traditional methods. This approach still presented challenges for the Critic's learning process, and it was evident that using GP alone was insufficient to completely overcome these limitations. Therefore, in the WGAN-GP model, both the Wasserstein distance and Gradient Penalty are utilized simultaneously to address these problems, ensuring stable gradients and continuous feedback during the training process.

Additionally, an analysis of the causes of color inconsistency revealed that the model struggled to achieve stable training, leading to occurrences of color inconsistency and degradation in image quality. In the WGAN-GP experiments, color consistency was a critical factor, and using a simple GP addition without the Wasserstein distance resulted in the Critic failing to provide adequate feedback, producing irregular or inconsistent color outcomes. These findings clearly illustrate the rationale for using the Wasserstein distance in the WGAN-GP model, demonstrating its superiority in delivering stable and consistent performance compared to traditional methods.

These ablation experiment results support the conclusion that the design of the WGAN-GP model offers superior training stability and image quality compared to conventional GAN-based approaches.

4.5. Comparison with Other Methods

The WGAN-GP-based color correction model proposed in this work was compared with existing histogram matching and color transfer techniques and was found to produce better results across various performance metrics.

Although histogram matching and color transfer techniques demonstrated some effectiveness in color matching, these methods were found to have limitations in reproducing the details of the overall image. In particular, histogram matching showed limitations in maintaining color consistency and resulted in information loss when compared to the

ground truth, especially in terms of texture and detail. The color transfer technique also exhibited limitations in maintaining the color consistency of the ground truth and was deficient in texture reproduction.

On the other hand, the proposed model achieved more natural color matching and texture reproduction as training progressed. In particular, the images generated by the mid-stage model not only showed good overall color matching but also reproduced textures that were fairly similar to the ground truth. At the end of training, the images generated by the model showed a slight decrease in color consistency compared to the mid-stage model. However, better results in texture reproduction were observed, which remained superior to the other methods, as shown in Figure 7.

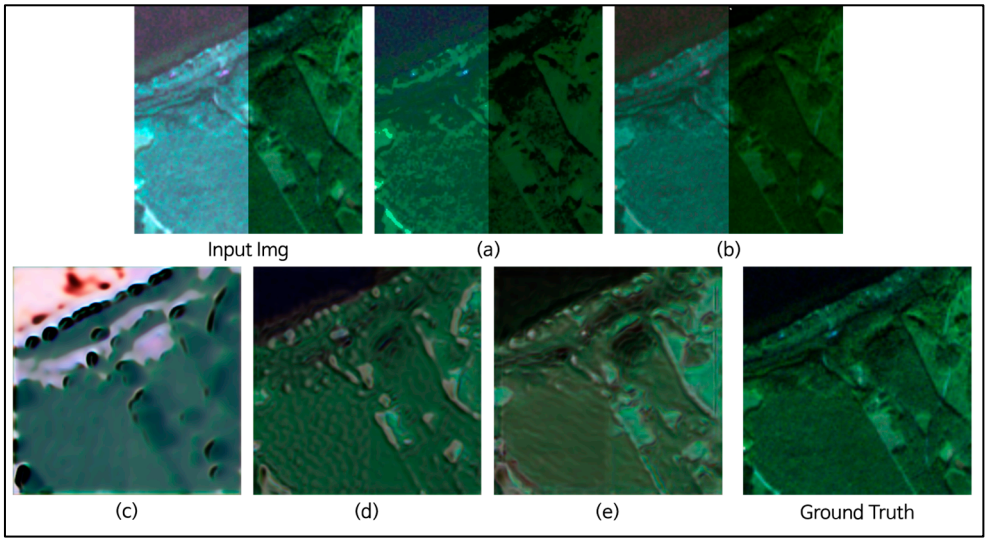

Figure 7. Comparison with other method's results. (**a**) Image processed using histogram matching, showing limitations in maintaining color consistency and significant information loss in texture and detail; (**b**) image processed using the color transfer technique, which also shows limitations in maintaining the ground truth's color consistency and lacks texture reproduction; (**c**) image generated by the early stage of the WGAN-GP-based model, where color distribution is irregular and texture representation is still underdeveloped; (**d**) image generated by the mid-stage model, demonstrating improved color matching and texture reproduction, with textures becoming more similar to the ground truth; and (**e**) image generated by the fully trained WGAN-GP model, showing a slight decrease in color consistency compared to the mid-stage model but offering superior texture reproduction compared to the other methods.

This architecture utilizes the Wasserstein distance and Gradient Penalty to enhance training stability and maintain color consistency while preserving the structural features of the image. These mechanisms allow the model to reduce color inconsistencies and enhance the structural integrity of the image, resulting in improved texture reproduction compared to traditional methods.

The quantitative analysis uses peak signal-to-noise ratio (PSNR) [27], structural similarity (SSIM) [28], CIE Delta E 2000 (CIEDE 2000) [29], and learned perceptual image patch similarity (LPIPS) [30] as evaluation metrics. PSNR directly reflects the pixel-level mean square error between the generated image and the original image; a higher value indicates less image distortion and a more accurate color distribution. SSIM measures the similarity between images based on brightness, contrast, and structure, reflecting the subjective quality of image restoration. The closer the SSIM value is to one, the more structurally similar the two images are, indicating better quality. CIEDE 2000 measures the color difference between two images, taking into account differences in hue, saturation, and lightness. A lower CIEDE 2000 value indicates less color difference between the two images and greater visual similarity. Compared to PSNR and SSIM, LPIPS is more aligned with

human perceptual judgment; a lower LPIPS value indicates a smaller perceptual difference between the generated image and the original image.

To provide a clearer understanding of these metrics, it is important to note that PSNR and SSIM are primarily focused on pixel-level accuracy and structural similarity, respectively, and may not fully capture the perceptual aspects of image quality as perceived by humans. This is where LPIPS becomes significant, as it evaluates perceptual similarity based on learned visual features, making it more relevant for assessing the quality of remote sensing images under varied conditions such as lighting or atmospheric effects. Additionally, CIEDE 2000 is particularly useful for assessing precise color differences, which is crucial when evaluating color correction algorithms. These metrics together provide a comprehensive assessment, balancing objective accuracy with perceptual quality.

In Table 1, the proposed method and other methods are evaluated using the specified performance metrics. The proposed method, particularly the mid-stage model of the WGAN-GP-based color correction model, demonstrates the best performance, showing optimal results across all metrics. This indicates that the proposed model can reproduce the colors and textures of the original image more accurately than existing methods.

Table 1. Evaluation of Histogram, Color Transfer, and Proposed Method.

Method	PSNR/dB	SSIM	CIEDE2000/Mean ΔE	LPIPS
Histogram Matching	27.5229	0.6949	9.4066	0.3194
Color Transfer	27.495	0.5585	9.8801	0.1933
Proposed Method (Early-Stage Model)	27.6841	0.4559	26.0101	0.6318
Proposed Method (Mid-Stage Model)	28.9298	0.7116	7.3487	0.3978
Proposed Method (Fully Trained Model)	28.2966	0.6459	9.6674	0.4005

Table 1 highlights that while the early-stage and fully trained models show variations in performance, the mid-stage model achieves the most balanced and optimal outcomes. This suggests that the mid-stage training phase effectively captures both color accuracy and texture details, demonstrating superior performance in high-quality image reproduction.

5. Discussion

A WGAN-GP-based color correction technique is proposed in this study to address the color correction problem of remote sensing images. To overcome the limitations of traditional methods, an approach using WGAN-GP is introduced that performs natural color correction while maintaining color consistency and the structural characteristics of the image.

The results show that the proposed WGAN-GP model can more consistently correct irregular color distributions and reproduce the texture and structure of images more precisely compared to existing methods. In particular, it performs well in preserving the structural elements of the target image while reflecting the style of the reference image during training.

However, as training progresses to the later stages, a slight decrease in color consistency is observed despite improvements in texture reproduction. This may be due to the model's increased focus on optimizing texture details over color accuracy, leading to a trade-off between these two aspects. Further adjustments in the loss function or model architecture may be necessary to achieve a more balanced performance in both color and texture preservation.

However, the purpose of this study is to enhance the visual quality of aviation simulators; therefore, additional research is needed regarding extreme weather and seasonal conditions. As the BigEarthNet-S2 dataset is post-processed to remove cloud cover, future studies will be conducted using Landsat or Sentinel tiles to explore these conditions further.

However, the proposed WGAN-GP-based approach has some limitations. It may be challenging to perfectly transfer the style of the reference image to the target image

by simply combining generators. To address this issue, it may be necessary to extend the research by incorporating additional models such as StyleGAN [31]. For example, StyleGAN's style transfer feature could be utilized to more precisely reflect the detailed style of the reference image in the target image. Additionally, it may be necessary to extend the Critic's structure to include a two-image comparison input that can more clearly identify differences between the reference image and the generated image, thereby enhancing the Critic's discrimination ability.

6. Conclusions

This study demonstrated that the WGAN-GP-based color correction technique enables more precise texture and structure reproduction in high-resolution remote sensing images compared to existing methods and can contribute to enhancing pilot immersion. In particular, the results suggest that the proposed method can significantly improve operational efficiency by saving time and cost compared to the ROK Air Force's existing manual processing methods, and this can be useful for generating training content based on various terrain images. Furthermore, this research is expected to expand the applicability of GAN-based technologies and advance the field of remote sensing image color correction. The proposed WGAN-GP model can contribute to solving practical problems in this field by delivering better performance than existing traditional methods.

This study shows that the proposed WGAN-GP model outperforms existing traditional methods and can more consistently correct irregular color distributions. Thus, the proposed method successfully improves the accuracy of color correction while preserving the structural characteristics of the image.

However, this study has some limitations. First, it may be difficult to perfectly transfer the style of the reference image to the target image by simply combining generators. Second, the structure of the Critic needs to be improved to more clearly distinguish between the reference image and the generated image. To overcome these limitations, future research should explore ways to further improve performance by combining additional models such as StyleGAN or extending the Critic's comparison structure.

This study makes an important contribution to the field of color correction for remote sensing images, and further validation in various environments and datasets will expand its applicability across different fields. Therefore, future research is needed to enhance the performance and expand the applicability of this model through additional experiments and validation in various environments. Based on these results, it is hoped that the proposed method will become a new standard for remote sensing image processing in the future.

Author Contributions: Conceptualization, C.L. and H.K.; Funding acquisition, D.S.; Methodology, C.L. and H.K.; Design of Scenario, H.C., J.C. and I.L.; Supervision, D.S.; Validation, B.K. and J.J.; Writing—original draft, C.L. and H.K.; Writing—review and editing, D.S. All authors have read and agreed to the published version of the manuscript.

Funding: This work was supported by the Challengeable Future Defense Technology Research and Development Program through the Agency For Defense Development(ADD) funded by the Defense Acquisition Program Administration(DAPA) in 2024 (No. 915073201).

Institutional Review Board Statement: Not applicable.

Informed Consent Statement: Not applicable.

Data Availability Statement: The original contributions presented in the study are included in the article; further inquiries can be directed to the corresponding author.

Conflicts of Interest: The authors declare no conflicts of interest.

References

1. Yaras, C.; Kassaw, K.; Huang, B.; Bardbury, K.; Malof, J.M. Randomized Histogram Matching: A Simple Augmentation for Unsupervised Domain Adaptation in Overhead Imagery. *IEEE J. Sel. Top. Appl. Earth Obs. Remote Sens.* **2024**, *17*, 1988–1998. [CrossRef]
2. Niu, H.; Lu, Q.; Wang, C. Color Correction Based on Histogram Matching and Polynomial Regression for Image Stitching. In Proceedings of the 2018 IEEE 3rd International Conference on Image, Vision and Computing (ICIVC), Chongqing, China, 27–29 June 2018; pp. 257–261.
3. Li, W.; Liu, X.; Yang, J.; Zhao, C.; Deng, H. A Color Correction Method Based on Incremental Multi-Level Iterative Histogram Matching. *IEEE Sens. J.* **2024**, *24*, 27892–27901. [CrossRef]
4. Grundland, M.; Dodgson, N.A. Color histogram specification by histogram warping. *Color Imaging X Process. Hardcopy Appl.* **2005**, *5667*, 610–621.
5. Li, Z.; Jing, Z.; Yang, X.; Sun, S. Color transfer based remote sensing image fusion using non-separable wavelet frame transform. *Pattern. Recog. Lett.* **2005**, *26*, 2006–2014. [CrossRef]
6. Xiao, X.Z.; Ma, L.Z. Color transfer in correlated color space. In Proceedings of the 2006 ACM International Conference on Virtual Reality Continuum and Its Applications (VRCIA'06), New York, NY, USA, 12–26 June 2006; pp. 305–309.
7. Pouli, T.; Reinhard, E. Progressive color transfer for images of arbitrary dynamic range. *Comput. Graph.* **2011**, *35*, 67–80. [CrossRef]
8. Tai, Y.W.; Jia, J.; Tang, C.K. Local Color Transfer via Probabilistic Segmentation by Expectation-Maximization. In Proceedings of the 2005 IEEE Computer Society Conference on Computer Vision and Pattern Recognition, CVPR 2005, San Diego, CA, USA, 20–26 June 2005; Volume I.
9. Fabbri, C.; Islam, M.J.; Sattar, J. Enhancing underwater imagery using generative adversarial networks. In Proceedings of the 2018 IEEE International Conference on Robotics and Automation(ICRA), Brisbane, Australia, 21–25 May 2018; pp. 7159–7165.
10. Liu, X.; Gao, Z.; Chen, B.M. MLFcGAN: Multilevel feature fusion-based conditional gan for underwater image color correction. *IEEE Geosci. Remote Sens. Lett.* **2019**, *17*, 1488–1492. [CrossRef]
11. Li, J.; Skinner, K.A.; Eustice, R.M.; Johnson-Roberson, M. Watergan: Unsupervised generative network to enable real-time color correction of monocular underwater images. *IEEE Robot. Autom. Lett.* **2017**, *3*, 387–394. [CrossRef]
12. Wang, N.; Zhou, Y.; Han, F.; Zhu, H.; Zheng, Y. UWGAN: Underwater GAN for real-world underwater color restoration and dehazing. *arXiv* **2019**, arXiv:1912.10269.
13. Yang, F.H.; Guo, R.R.; Cheung, R.C.; Lau, C.P. F-GAN: Real-Time Color Correction Model of Underwater Images. In Proceedings of the TENCON 2022—2022 IEEE Region 10 Conference (TENCON), Hong Kong, China, 1–4 November 2022; pp. 1–6.
14. Gulrajani, I.; Ahmed, F.; Arjovsky, M.; Dumoulin, V.; Courville, A.C. Improved training of wasserstein gans. In *Advances in Neural Information Processing Systems 30 (NIPS 2017)*; NeurIPS: Granada, Spain, 2017; pp. 5767–5777.
15. Arjovsky, M.; Chintala, S.; Bottou, L. Wasserstein gan. *arXiv* **2017**, arXiv:1701.07875.
16. Nyberg, D. *Exploring the Capabilities of Generative Adversarial Networks in Remote Sensing Applications*; Linkoping University Electronic Press: Linkoping, Sweden, 2021.
17. Clasen, K.N.; Hackel, L.; Burgert, T.; Sumbul, G.; Demir, B.; Markl, V. reBEN: Refined BigEarthNet Dataset for Remote Sensing Image Analysis. *arXiv* **2024**, arXiv:2407.03653.
18. Hong, Z.; Xu, C.; Tong, X.; Liu, S.; Zhou, R.; Pan, H.; Zhang, Y.; Han, Y.; Wang, J.; Yang, S. Efficient Global Color, Luminance, and Contrast Consistency Optimization for Multiple Remote Sensing Images. *IEEE J. Sel. Top. Appl. Earth Obs. Remote Sens.* **2023**, *16*, 622–637. [CrossRef]
19. Fan, C.; Chen, X.; Zhong, L.; Zhou, M.; Shi, Y.; Duan, Y. Improved Wallis Dodging Algorithm for Large-Scale Super-Resolution Reconstruction Remote Sensing Images. *Sensors* **2017**, *17*, 623. [CrossRef] [PubMed]
20. Sun, M.; Zhanga, J. Dodging Research for Digital Aerial Images. *Int. Arch. Photogramm. Remote Sens. Spat. Inf. Sci.* **2008**, *XXXVIIPar*, 349–354.
21. Morovic, J.; Sun, P.-L. Accurate 3d image colour histogram transformation. *Pattern Recognit. Lett.* **2003**, *24*, 1725–1735. [CrossRef]
22. Neumann, L.; Neumann, A. Color style transfer techniques using hue, lightness and saturation histogram matching. In Proceedings of the Computational Aesthetics in Graphics, Visualization and Imaging, Girona, Spain, 18–20 May 2005; pp. 111–122.
23. Reinhard, E.; Adhikhmin, M.; Gooch, B.; Shirley, P. Color transfer between images. *IEEE Comput. Graph. Appl.* **2001**, *21*, 34–41. [CrossRef]
24. Pitie, F.; Kokaram, A.C.; Dahyot, R. N-dimensional probability density function transfer and its application to color transfer. In Proceedings of the Tenth IEEE International Conference on Computer Vision, Beijing, China, 17–21 October 2005; pp. 1434–1439.
25. Katayama, T.; Song, T.; Shimamoto, T.; Jiang, X. GAN-based Color Correction for Underwater Object Detection. In Proceedings of the OCEANS 2019 MTS/IEEE SEATTLE, Seattle, WA, USA, 27–31 October 2019; pp. 1–4. [CrossRef]
26. Afifi, M.; Brubaker, M.A.; Brown, M.S. HistoGAN: Controlling Colors of GAN-Generated and Real Images via Color Histograms. In Proceedings of the 2021 IEEE/CVF Conference on Computer Vision and Pattern Recognition (CVPR), Nashville, TN, USA, 20–25 June 2021; pp. 7937–7946. [CrossRef]
27. Jason, A. Colorizing and Restoring Photo and Video. Available online: https://github.com/jantic/DeOldify (accessed on 16 January 2022).

28. Wang, Z.; Bovik, A.C.; Sheikh, H.R.; Simoncelli, E.P. Image quality assessment: From error visibility to structural similarity. *IEEE Trans. Image Process.* **2004**, *13*, 600–612. [CrossRef] [PubMed]
29. Sharma, G.; Wu, W.; Dalal, E.N. The CIEDE2000 color-difference formula: Implementation notes, supplementary test data, and mathematical observations. *Color Res. Appl.* **2005**, *30*, 21–30. [CrossRef]
30. Zhang, R.; Isola, P.; Efros, A.A.; Shechtman, E.; Wang, O. The Unreasonable Effectiveness of Deep Features as a Perceptual Metric. In Proceedings of the 2018 IEEE Conference on Computer Vision and Pattern Recognition, Salt Lake City, UT, USA, 18–23 June 2018; pp. 586–595.
31. Karras, T.; Laine, S.; Aila, T. A style-based generator architecture for generative adversarial networks. In Proceedings of the IEEE/CVF Conference on Computer Vision and Pattern Recognition (CVPR), Long Beach, CA, USA, 15–20 June 2019; pp. 4401–4410.